

A Study on the Potential of Sand Liquefaction Hazard at Chukai Sentral, Terengganu Using Plaxis 2D

Siti Fatimah Sadikon*, Nurul Ashikin Eshri & Juliana Idrus

Center for Civil Engineering studies, Universiti Teknologi MARA, Cawangan Pulau Pinang, Permatang Pauh Campus, 13500 Bukit Mertajam, Pulau Pinang, Malaysia

*Corresponding author: sitifatimah@uitm.edu.my

Received 17 April 2023, Received in revised form 6 August 2023

Accepted 30 October 2023, Available online 30 January 2024

ABSTRACT

An earthquake is classified as a natural disaster of mother nature. Sometimes, it cannot be predicted when it will occur and difficult to estimate the striking force values and the period of incident. The effect of the earthquake may catastrophic if the magnitude is more than 6 Richter. It had been proved by previous event, an earthquake could cause a huge impact towards the soil condition especially when the saturated soil is soft or loose since the propagation of shear wave and compression could induced the soil liquefaction and gave an effect towards excess pore pressure and effective stress of the soil that may affect the stability of infrastructure such as dam, embankment, and bridge. This study was conducted to analyse the horizontal displacement of soil due to earthquake and to evaluate the possibility of liquefaction at Chukai Sentral, Kemaman, Terengganu, Malaysia. The study was conducted using Plaxis-2D software based on Mohr-Coulomb soil model at magnitude of 5.4 Richter. The Mohr-Coulomb model was selected as its failure occurs when the shear stress acting on the soil reaches a critical value and the shear strength is related to the effective stress acting on it. The analysis was concentrated on the mesh deformation and horizontal displacement. The result shows the mesh deformation and horizontal displacement obtained in the boreholes not more than 6 mm. It is considered as a small deformation and will not trigger to the potential of liquefaction to that area. It can be concluded that the earthquake magnitude of 5.4 Richter is unable to disturb the natural resistance of the soil and structure due to their stiff layer proportion.

Keywords: Liquefaction; Plaxis 2D; Horizontal displacement

INTRODUCTION

Earthquake is the worst geological catastrophe that can cause ground shaking, soil failure, structure failure and even loss of life. Fortunately, Malaysia with its tectonically stable location has only recorded few and minor strikes of earthquake force. Currently, Peninsular Malaysia has recorded few data by experiencing shaking force (Shuib et al. 2017; Nazaruddin & Duerrast 2021) due to nearby active tectonic and fault rupture especially Sumatra Fault Zone and Sunda Plate. Due to the nearby active activity of "Ring of Fire", it is possible to estimate huge magnitude of an earthquake from the active plate and fault friction that could potentially cause Malaysia towards seismic risk. Seismic force propagation in soil might lead towards soil

failure especially liquefaction. Liquefaction happens when the pore water pressure in soil layer rapidly changes during a brief period when the soil layer is struck by the shaking amplitude produced by an earthquake epicenter. Changes in pore water pressure are influenced by the transmitting wave frequency and period, as well as the decreasing in soil strength and effective stress.

Liquefaction is the phenomenon in which the shear strength or stiffness of the soil diminishes due to sudden increase of pore water pressure and reduction of mean effective stress in the saturated cohesionless soil during the earthquake ground motion. Due to reduction of strength and the increase of capillary between the soil particle, the soil will experience floating and displaced horizontally. Referring to Lu et al. (2020), soil liquefaction can occur when the strength and stiffness of the soil are diminished

due to two changes of stress situation, and this phenomenon might impact structural settling after an earthquake.

Earthquake data from the databases of the international and national seismological centers, i.e., the International Seismological Center (ISC), European Mediterranean Seismological Center (EMSC), and the Malaysian National Seismic Network, which is operated by the Malaysian Meteorological Department (MMD or MetMalaysia) show that at least 59 earthquake events were recorded in Peninsular Malaysia from 1922 to 2020 (Nazaruddin & Duerrast, 2021) which came from Sumatra Subduction Zone and Sumatra Fault Zone with various magnitude from 5.2 to 9.0 (Marto et al. 2013). Another significant earthquake experienced again in Malaysia could give an impact of solid tremors by ground shaking, surface rupture, liquefaction, and tsunamis. However, from the literature, there were limited studies on liquefaction issues in Malaysia. Hence, this study was conducted to analyse the horizontal displacement in soil due to shaking force of 5.4 Richter and to evaluate the possibility of liquefaction in the east coast of Peninsular Malaysia.

METHODOLOGY

RESEARCH LOCATION AND MATERIAL PROPERTIES OF SOIL MODEL

The soil profile and properties were obtained from Site Investigation (SI) report of the construction project at Chukai Sentral, Kemaman, Terengganu. Five boreholes reports were used to identify the soil strata in which every borehole has different soil layer and thickness at the depth of 30m downwards from the ground surface as shown in Figure 1. From that figure, it is identified that the area is monopolized by clay and sand layer. It is obvious that there are two layers of sand in this area where the first sand layer is located between silt and clay while the second layer is located below the clay. The soil parameters were also extracted from the SI report and summarized as in Table 1 together with few additional soil properties used in the analysis.

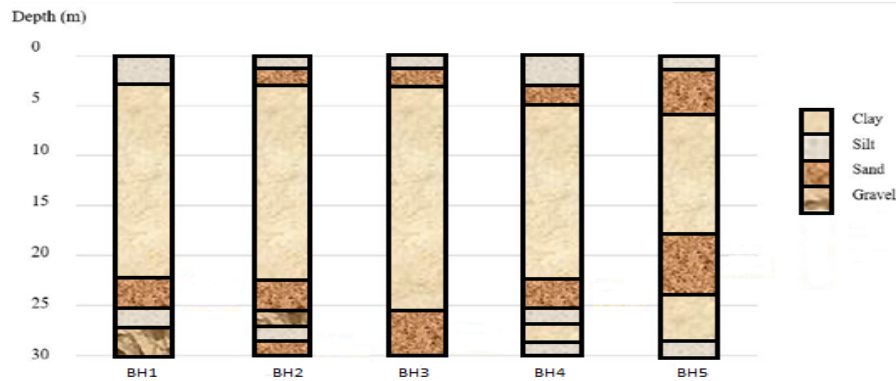


FIGURE 1. Soil profile in five boreholes at study area

TABLE 1. Soil properties used in the analysis

Soil parameter	Symbol	Soil type				Unit
		Clay	Silt	Sand	Gravel	
Unit weight above phreatic line	γ_{unsat}	16.00	16.84	17.00	11.63	kN/m ³
Unit weight below phreatic line	γ_{sat}	18.00	17.70	20.00	13.68	kN/m ³
Young's modulus	E_{re}	10,000	8,000	13,000	25,000	kN/m ²
Oedometer modulus	E_{oed}	16,050	1,077	17,500	25,000	kN/m ²
Poisson's ratio	ν	0.35	0.30	0.3	0	-
Cohesion	C	5.00	16.50	1.00	0.10	kN/m ²
Friction angle	ϕ	25.00	30.00	31.00	32.00	°
Dilatancy angle	ψ	0.00	-	0.00	0.00	°
Interface strength reduction	R_{inter}	0.50	1.00	1.00	1.00	-

PLAXIS 2D

Finite element method adopted in this study was Plaxis-2D software. The soil profile was subjected with the earthquake multiplier. The Mohr-Coulomb soil model was adopted due to its suitability in evaluating the plasticity that occurs in computation and the yield function due to force applied load. According to Wheeler et al. (2003) and Robert (2017), Mohr-Coulomb soil model is helpful in detecting displacement events in soil. Thus, in this study, Mohr-Coulomb elastic-plastic model was used to analyse the liquefy behaviour by determining the horizontal displacement of the soil.

The accelerogram data used for the evaluation of the earthquake at Chukai Sentral, Kemaman, Terengganu were compiled from accelerogram data in Strong Motion CD (smc) format of earthquake struck Upland, California on February 28th, 1990 at magnitude 5.4. This earthquake magnitude is the same as the maximum values of quakes that struck Terengganu at 10km/hr on March 15th, 2019 (Volcano Discovery, 2023). Hence, the smc format was adopted to evaluate the liquefaction hazard analysis at Chukai Sentral, Kemaman, Terengganu.

Developing the Plaxis-2D model was done by following the manual and the input parameter was carefully substituted into the input channel of the software analysis. In this study, the soil profile, soil characteristics and its original ground water level were preserved from SI report and secondary data adopted. Then, the soil profile analysis was run to get the result.

CONSTITUTIVE SOIL MOHR-COULOMB
MODEL ANALYSIS

Figure 2 shows the input sequence for completing the step forming the analysis according to the soil properties as stated in Table 1. The formation of model was initiated by inserting the requirement dimension of boundary, plotting the layer based on inserting coordinate and filling the required parameters on each of the soil types. When the soil profile was formed according to their layer as shown in Figure 1, the process was then continued with the setting of boundary types and the phreatic level (water level) for the soil profile. Standard boundary condition for earthquake was generated by using default setting. In the load menus by applying standard at the left and right vertical boundaries, earthquake boundaries automatically generated absorbent boundaries, as well as the prescribed $u_x=0.01$ m and $u_y=0.00$ m at the bottom boundary. For analysis section, the required multiplier was set according to the selected earthquake magnitude of 5.4 Richter (in smc format) and the calculation analysis was run.

After the analysis of the input data was completed, the output analysis screened out mesh deformation and horizontal displacement based on the shading contour on the soil profile diagram. Steps were repeated five times for five different boreholes. The complete steps of analysis are shown in Figure 2. Then, the results were evaluated to identify the possibility of soil liquefaction at that study area.

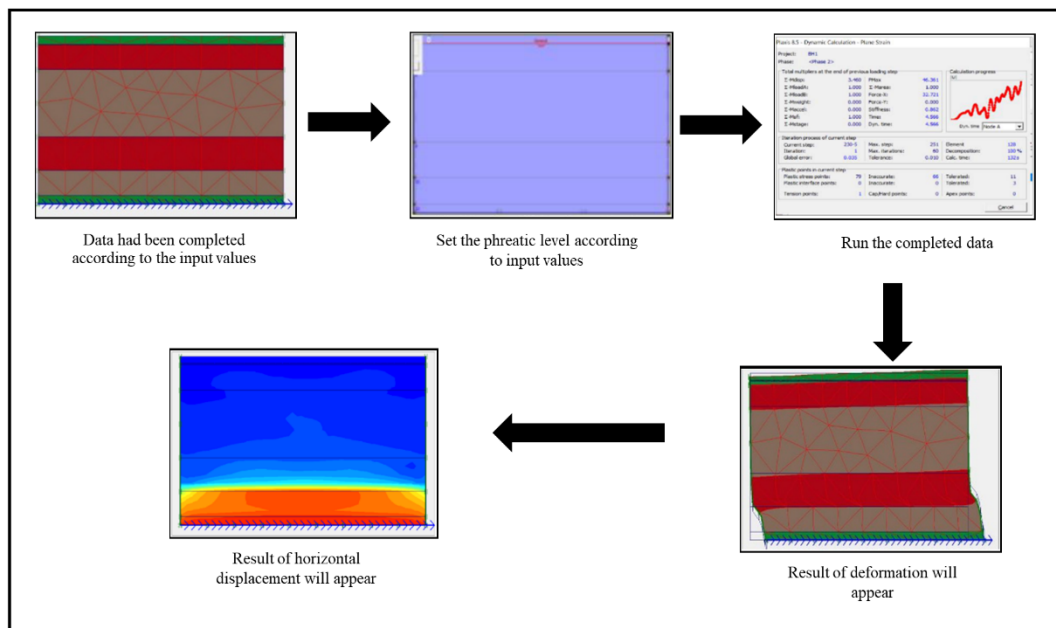


FIGURE 2. Workflow for constructive of soil Mohr-Coulomb model analysis

RESULTS AND DISCUSSION

MESH DEFORMATION

The initial mesh of the soil profile layer is the constant variable to analyse the degree of changes experienced by the soil profile when subjected to earthquake stimuli. Five mesh formations model were developed with an unsimilar layer of soil in 30.0 m depth as stated in borelog report. Then, the model was executed to analyse the result after the soil profile layer was subjected to earthquake forces.

The result of soil mesh deformation in five boreholes using Plaxis 2D is shown in Figure 3 as a compilation of difference generation state of mesh condition, pre-earthquake and post-earthquake in which the global coarseness was set to coarse. From the connection of mesh nodes of soil profile, little to moderate mesh deformation occurred when the soil profile was being subjected to an earthquake force. From the deformation mesh, Borehole 2 seems the most significant while Borehole 1 shows the less deformation compared to others.

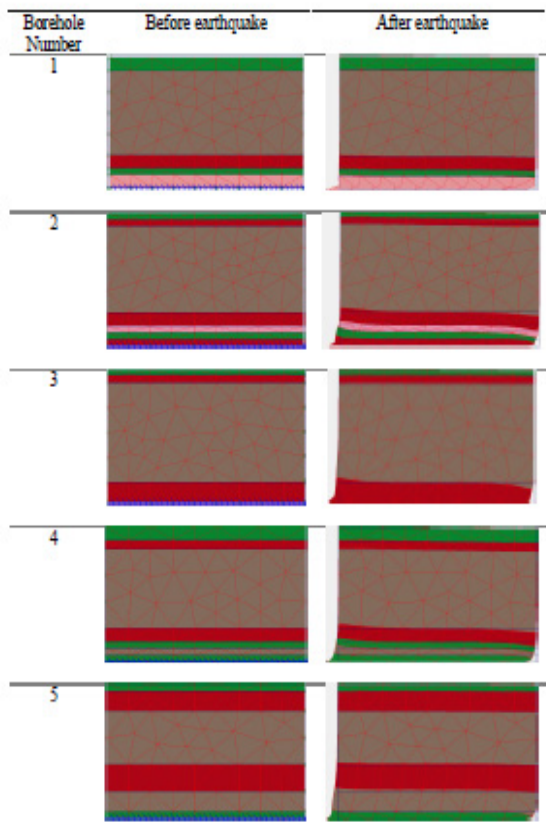


FIGURE 3. Change in mesh due to earthquake force

HORIZONTAL DISPLACEMENT

The horizontal displacement at five boreholes was analysed and the results are shown in Figure 4 to Figure 8.

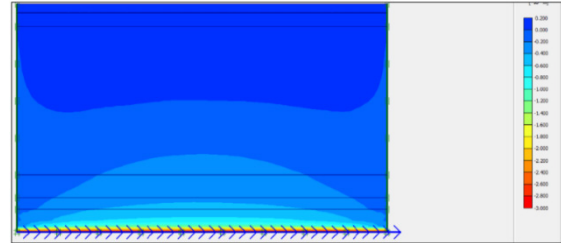


FIGURE 4. Horizontal displacement shading diagram of Borehole 1.

From Figure 4, the result of maximum horizontal displacement of Borehole 1 was 2.93 mm in gravel layer at 27.0 to 30.0 m depth. Meanwhile, the sand layer located at 22.5 to 25.5 m depth shows that the horizontal displacement was 1.00 mm. At the depth of 0 to 3.0 m and 3 to 22.5 m of silt and clay layer, it shows the least significant horizontal displacement at the range of 0 to 0.60 mm.

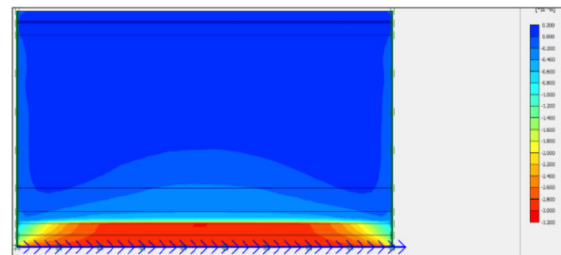


FIGURE 5. Horizontal displacement shading diagram of Borehole 2.

The maximum horizontal displacement in Borehole 2 was 3.00 mm at the depth of 27.0 to 30.0 m as shown in Figure 5. At this depth, it consists of silt and sand layer. Meanwhile, gravel layer at 25.5 to 27.0 m depth shows that the displacement was approximately 0.80 mm. At 22.5 to 25.5 m depth, it indicates that the horizontal displacement was 1.0 mm and upper layer continuously decreased to 0.2 mm which consisted of silt (0 to 1.5 m), sand (1.5 to 3.0 m) and clay layer (3.0 to 22.5 m).

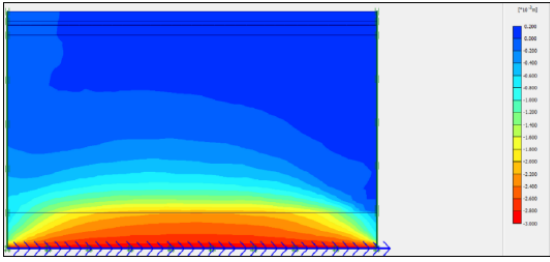


FIGURE 6. Horizontal displacement shading diagram of Borehole 3.

At Borehole 3 (Figure 6), the maximum horizontal displacement was 2.92 mm at the depth of 25.5 to 30.0 m of sand layer. Meanwhile, clay layer at depth of 3 to 25.5 m shows that the horizontal displacement was in the range of 0.2 mm to 1.8 mm. The upper layer at 0 to 1.2 m indicates silt had no horizontal displacement but another sand layer at depth of 1.2 to 3.0 m shows the horizontal displacement was 0.1 mm.

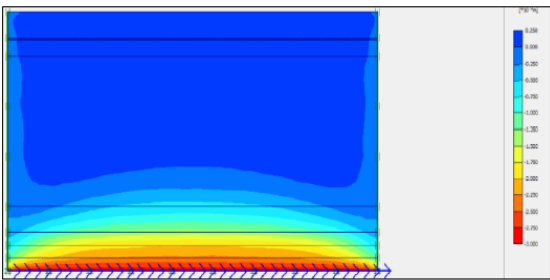


FIGURE 7. Horizontal displacement shading diagram of Borehole 4.

The maximum horizontal displacement at Borehole 4 was identified as 2.9 mm of layer of silt at 28.5 to 30.0 m depth. Meanwhile, sand layer at 22.5 to 25.5 m depth shows that the horizontal displacement was at the range of 0.75 to 2.25 mm. However, no horizontal displacement occurred at other depths as shown in Figure 7.

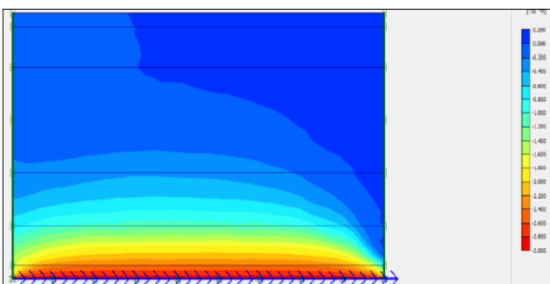


FIGURE 8. Horizontal displacement shading diagram of Borehole 5.

Finally, the maximum horizontal displacement in Borehole 5 occurred at the thin layer of silt in the depth of 28.5 to 30.0 m where it displaced 2.92 mm. The clay layer at 24 to 28.5 m depth was displaced between 1.0 to 2.2 mm while the sand layer at 18.0 to 24.0 m depth showed that its values were in the range of 0.6 to 1.4 mm. Meanwhile, the clay layer at 6.0 to 18.0 m depth showed a displacement of 0.2 to 0.8 mm only. The upper part that consisted of silt (0 to 1.5 m) and sand (1.5 to 6.0 m) had horizontal displacement in the range of 0.2 to 0.4 mm only as in Figure 8.

Liquefaction is specified as the secondary effect due to earthquake lateral shaking force. Based on the research by Othman and Marto (2019), some of the factors that trigger liquefaction are soil type and particle size distribution of soil. Hence, according to the mesh generation and deformation in Figure 3, the soil profile which has the highest proportion of cohesionless soil is more susceptible to liquefy. It could also be seen through the deformation mesh which had a slight difference of mesh and nodes throughout the soil profile layout after the model was subjected with representative of earthquake lateral force. The results are important as it entitles the potential of liquefaction hazard at Chukai Sentral, Kemaman, Terengganu by exploiting the values of horizontal movement corresponding to the subsoil profile. Cohesionless soil plays the major role in influencing the movement of the soil layer when it is subjected to an earthquake lateral force.

The graph of horizontal displacement at five different boreholes is presented in Figure 9. The flow of the graph shows the movement triggered by the shaking force from the earthquake in which the maximum values were found in different nodes (position of horizontal and vertical nodes) due to the acceptance of shaking force through the layer travel from the sources of the earthquake at the datum. This phenomenon can also be related to the relationship of cohesionless soil with the source of the shaking force, which means the higher proportion of sand or gravel in the profile layer, the more to lose of strength. Therefore, this analysis is concentrated on the second sand layer of soil profile at Chukai Sentral, Kemaman, Terengganu which has higher chances to be liquefied since the result is severe compared to the first layer.

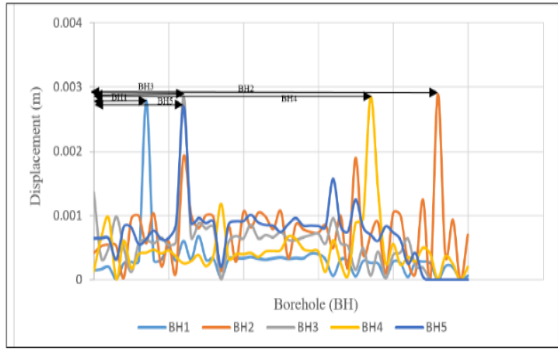


FIGURE 9. Horizontal displacement at five boreholes.

Table 2 shows the maximum value of horizontal displacement at the second sand layer from each borehole as explained. It shows that Borehole 2 has the highest displacement compared to other boreholes.

The maximum values of horizontal displacement were denoted beneath the breakwater. It was easy to observe the least significant value that showed higher magnitude of displacement since the value was very small. Consequently, it is noticeable that the result indicates the subsoil layer for Borehole 2 shows the highest horizontal displacement among boreholes where it displaced at about 3.0 mm.

TABLE 2. Maximum horizontal displacement at five boreholes

Borehole number	Depth of sand layer from ground level (m)	Horizontal displacement (mm)
1	22.5 – 25.5	1.00
2	28.5 – 30.0	3.00
3	25.5 – 30.00	2.92
4	22.5 – 25.5	2.25
5	18.0 – 24.0	1.40

However, the horizontal displacement at Borehole 1, 3, 4 and 5 showed less value. It is because the composition of the cohesionless soil in Borehole 2 was composed of the highest percentage of sand at 63% compared to Borehole 1, 3, 4 and 5 with the percentages of 24%, 49%, 45% and 16% respectively. This percentage of soil composition was found from the sieving test analysis in SI report. The highest percentage of cohesionless soil in the soil profile makes it more significant towards the contribution of lateral displacement.

TENDENCY OF SOIL LIQUEFACTION

The key layer identification criterion aims to discover the soil layer that is most prone to cause and exhibit liquefaction at the ground surface for a certain site (Zhou et al. 2020).

Based on the results of displacement in five boreholes, Borehole 2 showed the higher deformation compared to 4 other boreholes due to the layering of the soil in 30.0 m depth. Alternate layering of sand in the soil profile and composition of gravel at 1.5 m depth contributes to the element of drainage that gives space to water to sneak between soil particles and break the bond resulting into the drastic decrease of the shear strength of the soil. On the other hand, it showed that the least mesh deformation due to thick clay layer and the shifting of soil types in the 30.0 m depth was not significant with the cohesionless soil.

Overall, from the soil profile of up to 30.0 m depth, Borehole 1 to Borehole 5 showed that the thickness of the cohesive soil (clay layer) varied, starting from 4.5 m to 22.2 m depth as shown in Figure 1. Compared to cohesionless soil, it is prone towards liquefaction which was recorded at 1.5 m until 4.5 m thickness. Through the difference ratio of the composition of cohesive and cohesionless soil, it is an earlier sign which proves that soil layer at Chukai Sentral, Kemaman, Terengganu consists of cohesive soil. It already has the properties to resist the break of shear stress because of pore water pressure increment and reduction of mean effective stress due to sudden loading of an earthquake lateral shaking force that contributes to the results obtained. To strengthen the statement, Figure 10 shows the proposed range of grain size distribution for potentially liquefiable soil and most liquefiable soil (Othman & Marto, 2019).

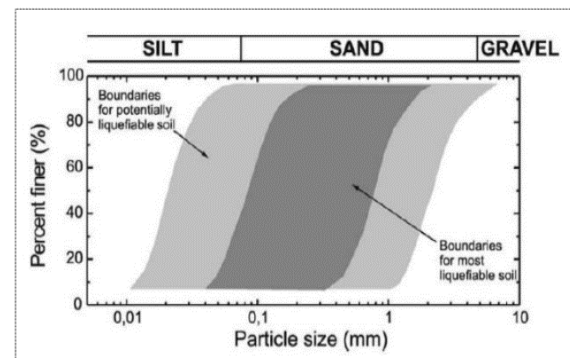


FIGURE 10. Grain Size Distribution Boundaries for Liquefaction (Othman & Marto, 2019).

According to Wang et al. (2012), liquefaction induces ground lateral flow of saturated soil. According to the analysis procedure of 30.0 m depth of the soil profile, the initial phreatic level (water level) in the five-borehole location was significantly below ground surface with the range of 1.21 to 3.23 m. That means, all the cohesionless layer was in fully saturated condition. However, the result showed that there was very minimum horizontal displacement although cohesionless soil was saturated.

When the earthquake strikes saturated soils, the water-filled pore spaces collapse, reducing the overall volume of the soil. From the result of horizontal displacement at sand layer in all five boreholes, it shows that the deformation is too small to trigger the possibility of the soil to liquefy. Usually, liquefaction will occur if the horizontal deformation is more than 530 mm (Ozutsumi et al. 2010). Thus, it secures the original soil layer from being restructured by liquefaction during and after the earthquake.

CONCLUSION

Simulation was aimed to assess the horizontal displacement of the soil as well as to evaluate the soil ability to liquefy. This study was able to understand the behaviour of soil in Malaysia, which discovers that the soil in Malaysia can absolutely resist liquefaction particularly at Chukai Sentral, Kemaman, Terengganu when being induced by magnitude of earthquake at 5.4 Richter using Plaxis-2D simulation. It was found that the least propensity of liquefaction is due to low values of horizontal displacement. Furthermore, the five boreholes indicated that the soil layer is too stiff and solid to contribute ground failure due to ground shaking. Furthermore, the composition of cohesionless soil in the research area is less than cohesive soil. As a result, this study contributes knowledge on the layering state of the soil which also plays a role in increasing the strength of the soil and resisting rupture when a shaking force is applied to the ground layer.

ACKNOWLEDGEMENT

The authors would like to thank the Center for Civil Engineering studies, Universiti Teknologi MARA Cawangan Pulau Pinang for the use of services and facilities in conducting the research which leads to this paper and the financial support in publishing this paper.

DECLARATION OF COMPETING INTEREST

None

REFERENCES

- Bahari, B., Hwang, W., Kim, T. H., & Song, Y. S. 2020. Estimation of liquefaction potential in EcoDelta City (Busan) using different approaches with effect of fines content. *International Journal of Geo-Engineering* 11(1): <https://doi.org/10.1186/s40703-020-00121-4>
- Beatty, M. H., & Perlea, V. G. 2011. Several observations on advanced analyses with liquefiable materials. *Thirty First Annual USSD Conference on 21st Century Dam Design-Advances and Adaptations. San Diego, California, April 2011*, 11–15.
- Daftari, A., & Kudla, W. 2014. Prediction of Soil Liquefaction by Using UBC3D-PLM Model in PLAXIS. *International Journal of Civil and Environmental Engineering*, 8(2): 106–111. <http://waset.org/publications/9997544>
- Hashim, M. S. and R. H. 2017. Preliminary study of soil liquefaction hazard at Terengganu shoreline, Peninsular Malaysia <https://doi.org/10.1088/1757-899X/210/1/012020>
- Hashim, Huzaifa, Suhatri, M., Hashim, R., & Suhatri, M. 2017. Assessment of liquefaction hazard along shoreline areas of Peninsular Malaysia. 5705. <https://doi.org/10.1080/19475705.2017.1391882>
- Hazreek, M., Abidin, Z., Saad, R., & Ahmad, F. 2012. Seismic Refraction Investigation on Near Surface Landslides at the Kundasang area in Sabah, Malaysia. 50 (ICASCE): 516–531. <https://doi.org/10.1016/j.proeng.2012.10.057>
- Hazreek, M., Abidin, Z., Tun, U., Onn, H., Saad, R., Ahmad, F., Wijeyesekera, D., Tun, U., & Onn, H. 2012. Integral Analysis of Geoelectrical (Resistivity) and Geotechnical (SPT) Data in Integral Analysis of Geoelectrical (Resistivity) and Geotechnical (SPT) Data in Slope Stability Assessment. May 2014.
- Hu, Q., Zhang, J. M., & Wang, R. 2020. Quantification of dilatancy during undrained cyclic loading and liquefaction. *Computers and Geotechnics* 128(6): 103853. <https://doi.org/10.1016/j.compgeo.2020.103853>
- Jainih, V., and N. S. H. Harith. 2020. Seismic Vulnerability Assessment in Kota Kinabalu, Sabah. *IOP Conference Series: Earth and Environmental Science* 476(1). doi: 10.1088/1755-1315/476/1/012053.
- Lu, C. W., Chu, M. C., Ge, L., & Peng, K. S. 2020. Estimation of settlement after soil liquefaction for structures built on shallow foundations. *Soil Dynamics and Earthquake Engineering* 129(3): 105916. <https://doi.org/10.1016/j.soildyn.2019.105916>
- Marto, A., Tan, C. S., Kassim, F., & Mohd Yunus, N. Z. (2013). Seismic impact in Peninsular Malaysia. The 5th International Geotechnical Symposium-Incheon, May, 237–242. <https://doi.org/10.13140/2.1.3094.9129>
- Nazaruddin, Dony & Duerrast, Helmut. 2021. Intraplate earthquake occurrence and distribution in Peninsular Malaysia over the past 100 years. *SN Applied Sciences* 3. 10.1007/s42452-021-04686-2.

- Othman, B. A., & Marto, A. 2019. A liquefaction resistance of sand-fine mixtures: Short review with current research on factors influencing liquefaction resistance 7(3): 20–30.
- Ozutsumi, O., S. Sawada, and S. Iai. 2010. Analysis of Liquefaction Induced Residual Deformation for Two Types of Quay Walls Analysis By ‘Flip.’ *Proc. 12th World Conference on Earthquake Engineering, Auckland, New Zealand*
- Robert, D.J. & Thusyanthan, Indrasenan. 2017. Uplift resistance of buried pipelines in partially saturated sands. *Computers and Geotechnics* 97. 10.1016/j.compgeo.2017.12.010.
- Shuib, M., Manap, M., Tongkul, F., Abd Rahim, I. Jamaludin, T., Surip, N., Abu Bakar, R., Abas, M., Musa, R. and Ahmad, Z. 2017. Active faults in peninsular malaysia with emphasis on active geomorphic features of Bukit Tinggi region. *Malaysian Journal of Geosciences* 1: 13-26. 10.26480/mjg.01.2017.13.26.
- Toloza, P. V. 2018. Liquefaction Modelling using the PM4Sand Constitutive Model in PLAXIS 2D. MS.c. Thesis, Delft University of Technology.
- Volcano Discovery (2023) Volcano Discovery website. <https://www.volcanodiscovery.com/place/46147/earthquakes/marang.html>
- Wang, B., Zen, K., Chen, G. Q., & Kasama, K. 2012. Effects of excess pore pressure dissipation on liquefaction-induced ground deformation in 1-g shaking table test. *Geomechanics and Engineering*, 4(2), 91–103. <https://doi.org/10.12989/gae.2012.4.2.091>
- Wang, Yu, Wei, S., Wang, X., Lindsey, E. O., Tongkul, F., Tapponnier, P., Bradley, K., Chan, C. H., Hill, E. M., & Sieh, K. 2017. The 2015 M w 6.0 Mt. Kinabalu earthquake: an infrequent fault rupture within the Crocker fault system of East Malaysia. *Geoscience Letters*, 4(1). <https://doi.org/10.1186/s40562-017-0072-9>
- Weijie Loi, D., Eshwaraiyah Raghunandan, M., & Swamy, V. 2018. Revisiting seismic hazard assessment for Peninsular Malaysia using deterministic and probabilistic approaches. *Natural Hazards and Earth System Sciences* 18(9): 2387–2408. <https://doi.org/10.5194/nhess-18-2387-2018>
- Wheeler, S. & Sharma, Radhey & Buisson, M.. 2003. Coupling of hydraulic hysteresis and stress–strain behavior in unsaturated soils. *Geotechnique* 53: 41-54. 10.1680/geot.53.1.41.37252.
- Zhang, X., Li, X., & Xu, C. 2020. Study on the corrected hyperbolic model of liquefaction evaluation for. *Soil Dynamics and Earthquake Engineering* 139(9): 106424. <https://doi.org/10.1016/j.soildyn.2020.106424>
- Zhou, Y., Xia, P., Ling, D., & Chen, Y. 2020. Datasets for liquefaction case studies of gravelly soils during the 2008 Wenchuan earthquake. *Data in Brief* 32: 106308. <https://doi.org/10.1016/j.dib.2020.106308>